

Observations of Cosmic Ray Electrons and Positrons Using an Imaging Calorimeter

G. Basini³, B. Bongiorno³, M. T. Brunetti⁶, A. Codino⁶, R.L. Golden², C. Grimani², B.L. Kimbell², M. Menichelli⁶, A. Morselli¹, J.F. Ormes⁴, M.P. De Pascale¹, P. Picozza¹, M. Ricci³, I. Salvatori⁶, E. Seo⁴, P. Spillantini⁵, S.A. Stephens^{2,7}, R.E. Streitmatter⁴, S.J. Stochaj², W.R. Webber²

1. Dipartimento di Fisica and INFN dell' Universita' di Roma "Tor Vergata", Italy 2. New Mexico State University, New Mexico, US 3. INFN-Laboratori Nazionali di Frascati, Italy 4. NASA-Goddard Space Flight Center, Maryland, USA 5. Dipartimento di Fisica and INFN dell' Universita' di Firenze, Italy 6. Dipartimento di Fisica and INFN dell' Universita' di Perugia, Italy 7. Tata Institute of Fundamental Research, Bombay, India 8. Dipartimento di Fisica and INFN dell' Universita' di Roma, Italy

ABSTRACT

On Sept. 5, 1989 a balloon-borne magnet spectrometer system was flown for 5.5 hrs at an altitude of more than 117,000 ft altitude from Prince Albert Saskatchewan. The instrument incorporated a momentum spectrometer, a gas Cherenkov detector, a time-of-flight scintillator array and an imaging calorimeter, 6.4 radiation lengths thick. Inclusion of the calorimeter has allowed significant improvements in the ability to distinguish electrons and positrons from the other constituents of the cosmic rays. The electron flux was found to be $J_e = 109 \cdot E^{-(2.83 \pm 0.11)}$ electrons/m²-sr-sec-GeV in the energy range 2.5 - 20 GeV. The $e^+/(e^+ + e^-)$ ratio was (0.104 ± 0.022) in the energy range 4 - 10 GeV.

The Apparatus

Figure 1 shows the instrument. Signals from the Cherenkov detector and all scintillators (T1, T2, S1, T3, T4) were pulse-height analyzed. The Gas Cherenkov detector was filled with a 50-50 mixture of Freon-12 and Freon-22

giving it a threshold relativistic factor $\gamma = 23$. The maximum detectable magnetic rigidity (momentum/charge) was 118 GeV/c. Details of the magnet spectrometer and its performance are contained in Golden et al. 1991. The calorimeter consisted of 40 layers (20 in each of two orthogonal views) of 64 brass streamer tubes, for a total of 6.4 radiation lengths and 0.6 nuclear interaction lengths. Figure 2 shows calorimeter images for four different types of events. As one can see, the images for different interactions are quite distinct. Since the image data is gathered in digital form, algorithms can be applied directly to the data in order to perform non-subjective tests.

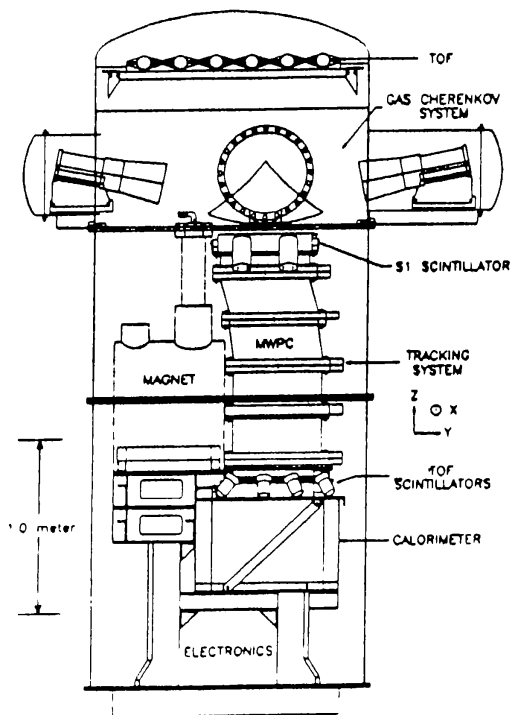


Figure 1. The Instrument.

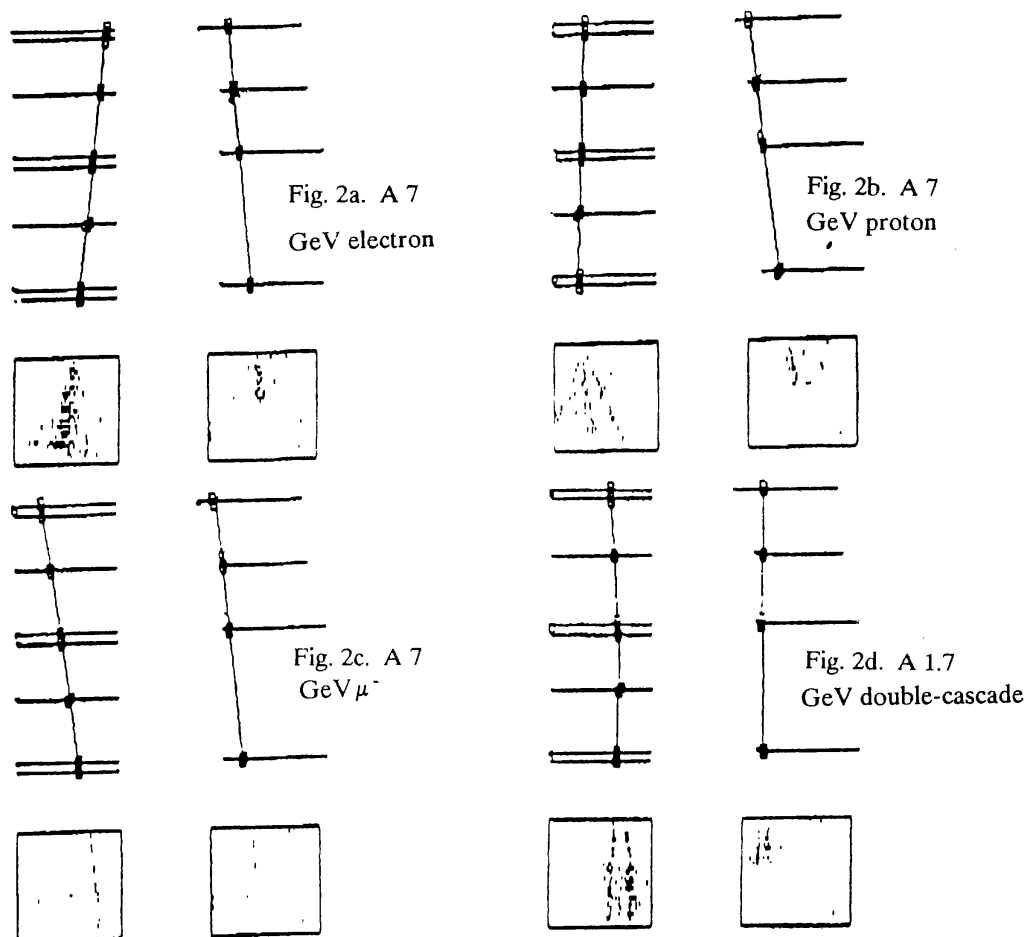


Figure 2. Images for 4 different types of events. Each figure shows the MWPC data and the calorimeter image. The left side of each view is the x-view where most of the bending takes place. The right half is the y-view. Note that the lower half of the y-view of the calorimeter was not operating during the flight.

The trigger for an event was a coincidence between T1, T2, T3 and T4. The S1 was then tested by the on-board computer to assure that the pulse-height was greater than $0.25 I_0$ (where I_0 corresponds to the pulse-height of a single minimum ionizing particle). Events surviving this test were transmitted to the ground.

Data Analysis

Selection of e^-

Negatively charged cosmic rays at balloon altitudes are principally μ^- , e^- and \bar{p} . Pions and kaons will have decayed before reaching the payload because secondary cosmic rays are

produced, on the average, 1 scale height (about 18 km) above the payload. The negative charge is established by the magnet spectrometer and responses of the Cherenkov detector and calorimeter are used to distinguish e^- from the other species. The selection criteria included (1) trajectory reconstruction and goodness of fit tests as described in Golden et al. 1991, (2) $|Z| < 1.8 I_0$, (3) Cherenkov output ≥ 1 p.e..

None of the events selected with criteria 1-3 showed interactions with wide angle secondaries or starting points below the first few layers in the calorimeter. Either of these characteristics would be indicative of the presence of hadrons. Instead, the remaining events fall into two distinct

categories (at energies above a few GeV): 1) a cascade is present, 2) no cascade present.

Below 20 GeV the only expected background of significance is due to m^- . Since the m^- are weakly interacting they produce a single straight track in the calorimeter. Electrons, on the other hand, produce electromagnetic showers. The lateral spread of these showers is about two Mollier radii (2×1.6 cm).

Shower recognition was quantified by projecting the fitted MWPC trajectory into the calorimeter and counting the number of planes in which multiple adjacent wires were triggered. A "shower cluster" is defined as a plane having two or more wires triggered within 5 wires of the extrapolated MWPC trajectory. Since the background and shower development are energy dependant, energy dependant selection criteria are used:

Test 4. Calor. requirement for e^- :

1.0-2.5 GeV, no calorimeter requirement
2.5-4.0 GeV, at least two planes show shower clusters
4.0-20.0 GeV, at least five planes show shower clusters

Selection of e^+

Selection of positrons is much more difficult than selection of electrons because of the presence of the large flux of protons. In order to obtain better background rejection a more strict calorimeter selection test was made:

Test 4. (for e^+)

At least 10 planes show shower-clusters.

This criterion is satisfied by 84% of the e^- in the interval 4-10 GeV. This efficiency is used in computing the $e^+/(e^+ + e^-)$ ratio. An inspection of the positron candidates passing these criteria reveals that all of the events showed cascades that started in the top 3 layers of the calorimeter.

The same criteria (1-3) were used for e^+ and e^- . The upper energy

limit for the e^+ observations was set at 10 GeV to eliminate contamination due to "spill-down" of protons above Cherenkov threshold. The lower energy limit was set at 4 GeV because the efficiency for passing test 4 rapidly declines at lower energies.

Results

electron results:

Figure 3 contains a summary of the e^- observations, along with data from previous experiments. The results of Tang's experiment have been divided by 1.1, because in that experiment there wasn't any possibility to distinguish electrons and positrons. Corrections have been included for bremsstrahlung losses above the spectrometer, for loss of events due to pair production in the spectrometer, albedo from the spectrometer, dead-time, and for electrons produced by hadronic interactions in the atmosphere. The flux at the top of the atmosphere was determined by finding the incident flux, which, when propagated to float altitude by using the cascade theory, best matches the flux observed at the payload.

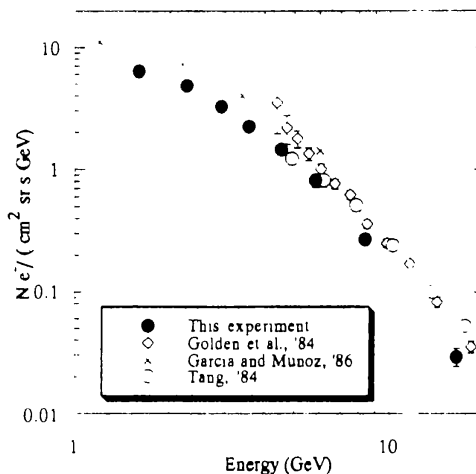


Figure 3. Electron fluxes. A fit, assuming that the flux is of the form $A \cdot E^{-\gamma}$ gives $J_{e^-} = 109 E^{-(2.83 \pm 0.11)}$ particles/m² sr sec.

positron results:

Fifteen events passing the e^+ selection criteria were found in the interval 4-10 GeV. Inspection of these events revealed that all had dense forward collimated cascades beginning in the top few layers. Were protons present in the sample roughly half of them would pass through the calorimeter without interacting, and the other half would give low multiplicity, wide angle cascades that started at various depths in the calorimeter. Since all observed cascades appear to be electromagnetic cascades, we conclude that no proton background is present. To our knowledge this is the first positron observation made without hadron background contamination. In Fig. 4 data from this and previous experiments are shown. In the energy range 4-10 GeV the ratio of $e^+ / (e^+ + e^-)$ is (0.104 ± 0.022) .

Discussion

Although the flight was short, it has yielded data of excellent quality. Unambiguous identification of both positrons and electrons has been accomplished. As the methods for quantitative topological separation using the calorimeter data are improved, the energy range over which separations can be performed will be increased. The observed rates agree well with our prior observations (Golden et al 1985) indicating that the earlier measurements were accurate in spite of large background subtractions.

References

- Agriner, B. et al., Lett. Nuovo Cimento ser. 1, 1, 53 (1969)
 Buffington, A., Orth, C. D., and Smoot, G. F., Ap. J., **199**, 699, (1975).
 Faneslow, J. L., Hartman, R. C., Hildebrand, R. H., and Meyer, P., Ap., J., 158, 771 (1969).
 Golden, R. L., S. Horan, B. G. Mauger, G. D. Badhwar, J. L. Lacy, S. A. Stephens, R. R. Daniel, and J. E. Zipse, Phys. Rev. Letters, 43, 1264 (1979).

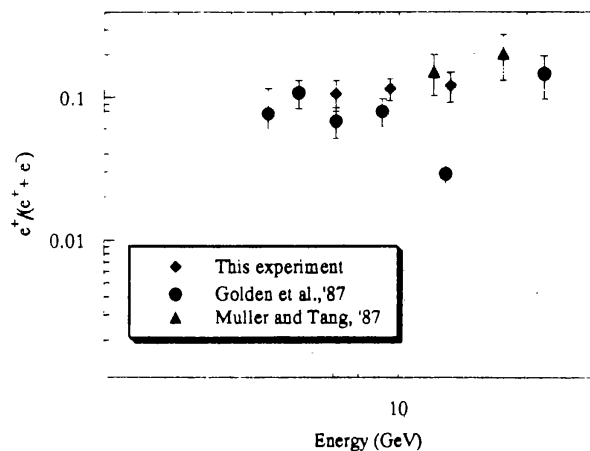


Figure 4. $e^+ / (e^+ + e^-)$ ratio measurement from this and previous experiments

- Golden, R. L., B. G. Mauger, G. D. Badhwar, R. R. Daniel, J. L. Lacy, and J. E. Zipse, Ap. J., **287**, 622 (1984).
 Golden, R. L., S. A. Stephens, B. G. Mauger, G. D. Badhwar, R. R. Daniel, S. Horan, J. L. Lacy, and J. E. Zipse, Astr. Ap., 188, 145 (1987).
 Golden, R. L., Grimani, C., Kimbell, B., Webber, W. R., Basini, G., Ricci, Morselli, A., M., Ormes, J., Seo, E. S., Stochaj, S., Streitmatter, R., Spillantini, P., Codino, A., Menichelli, M., DePascale, M. P., Picozza, P., Bongiorno, F., PAL technical note #223, available on request. To appear in Nucl. Instr. and Meth. (1991)
 Muller, D. and K. Tang, Ap. J., 312, 183 (1987).
 Nishimura J., Handbuch der physik, (Springer - Verlage, 1967), 46, 1.
 Nishimura et al., Proc. 17th Internat. Cosmic Ray Conf. (Paris), 2, 94 (1985)
 Tang, K., Ap. J., 278, 881 (1984)